Photooxidation of Diimine Dithiolate Platinium(II) Complexes Induced by Charge Transfer to Diimine Excitation

Yin Zhang, Kevin D. Ley, and Kirk S. Schanze*,†

Department of Chemistry, University of Florida, PO Box 117200, Gainesville, Florida 32611-7200

Received June 7, 1996[⊗]

A photochemical and photophysical investigation was carried out on (tbubpy)Pt^{II}(dpdt) and (tbubpy)Pt^{II}(edt) (**1** and **2**, respectively, where tbubpy = 4,4′-di-*tert*-butyl-2,2′-bipyridine, dpdt = *meso*-1,2-diphenyl-1,2-ethanedithiolate and edt = 1,2-ethanedithiolate). Luminescence and transient absorption studies reveal that these complexes feature a lowest excited state with $Pt(S)_2 \rightarrow$ tbubpy charge transfer to diimine character. Both complexes are photostable in deoxygenated solution; however, photolysis into the visible charge transfer band in air-saturated solution induces moderately efficient photooxidation. Photooxidation of **1** produces the dehydrogenation product (tbubpy)Pt^{II}-(1,2-diphenyl-1,2-ethenedithiolate) (**4**). By contrast, photooxidation of **2** produces S-oxygenated complexes in which one or both thiolate ligands are converted to sulfinate ($-SO_2R$) ligands. Mechanistic photochemical studies and transient absorption spectroscopy reveal that photooxidation occurs by (1) energy transfer from the charge transfer to diimine excited state of **1** to $^3O_2$ to produce $^1O_2$ and (2) reaction between $^1O_2$ and the ground state **1**. Kinetic data indicates that excited state **1** produces $^1O_2$ efficiently and that reaction between ground state **1** and $^1O_2$ occurs with $k \approx 3 \times 10^8$ M^{-1} s^{-1}.

Introduction

Transition metal−organic complexes display a rich array of spectroscopic transitions and long-lived excited states with charge transfer character.[1−3] Depending on the details of the electronic structure of the complex, inner sphere transitions having metal-to-ligand charge transfer (MLCT), ligand-to-metal charge transfer (LMCT), ligand-to-ligand charge transfer (LLCT), and intraligand charge transfer (ILCT) are observed.[4] A significant amount of work has been carried out to determine the factors that control the spectroscopic properties and photochemical reactivity of these charge transfer states.[1−7] Interest in this area has been driven by several factors, including the possibility for development of useful photosensitizers for optical to chemical energy conversion[8] and/or luminescent chemical sensors that may find application to chemical and biological problems.[9,10]

Although by far the most work on charge transfer excited states has focused on luminescent MLCT states in d^6 transition metal complexes containing diimine ligands,[5] recent work by Eisenberg and co-workers has drawn attention to the interesting properties of charge transfer states in mixed-ligand Pt(II) complexes that contain dithiolate electron donor and diimine electron acceptor ligands (i.e., (NN)Pt^{II}(SS)).[11−19] Through a series of detailed investigations this group has demonstrated that a wide range of (NN)Pt^{II}(SS) complexes display a solvatochromic absorption band in the mid-visible region and luminescence at room temperature in fluid solution.[11−19] The electronic state giving rise to the visible absorption band and the room temperature luminescence has been assigned as arising from a charge transfer transition from the HOMO that is delocalized over the $Pt(S)_2$ unit to the LUMO that is localized largely on the diimine acceptor ligand.[17,20,21] As such, the excited state has mixed LLCT and MLCT character, and has been termed charge transfer to diimine.[17,19]

While most of the work carried out to date on (NN)Pt^{II}(SS) complexes has focused on the photophysics of the charge transfer to diimine state, several recent reports suggest that the chromophore is also photochemically reactive in oxygenated solution. Thus, in a series of papers Srivastava and co-workers demonstrated that photolysis of (bpy)Pt^{II}(tdt) (bpy = 2,2′-bipyridine and tdt = 3,4-toluenedithiolate) and several related complexes in the presence of dioxygen leads to decomposition of the complex.[22−24] Although the products of the photodecomposition were not determined, several (NN)Pt^{II}(SS) complexes were found to sensitize $^1O_2$* with moderate efficiency.

† E-mail: kschanze@chem.ufl.edu.

⊗ Abstract published in *Advance ACS Abstracts,* November 1, 1996.

(1) *Concepts of Inorganic Photochemistry*; Adamson, A. W., Fleischauer, P. D., Eds.; Wiley: New York, 1975.
(2) Geoffroy, G. L.; Wrighton, M. S. *Organometallic Photochemistry*; Academic Press: New York, 1979.
(3) Ferraudi, G. *Elements of Inorganic Photochemistry*; Wiley: New York, 1988.
(4) Vogler, A.; Kunkely, H. *Comments Inorg. Chem.* **1990**, *9*, 201.
(5) Juris, A.; Balzani, V.; Barigelletti, F.; Campagna, S.; Belser, P.; von Zelewsky, A. *Coord. Chem. Rev.* **1988**, *84*, 85.
(6) Endicott, J. F. in ref 1, p 81.
(7) Meyer, T. J. *Prog. Inorg. Chem.* **1983**, *30*, 389.
(8) (a) *Energy Resources Through Photochemistry and Catalysis*; Grätzel, M., Ed.; Academic Press: New York, 1983. (b) Hagfeldt, A.; Grätzel, M. *Chem. Rev.* **1995**, *95*, 49.
(9) Demas, J. N.; DeGraff, B. A. *Anal. Chem.* **1991**, *63*, 829a.
(10) Pyle, A. M.; Barton, J. K. *Prog. Inorg. Chem.* **1990**, *38*, 412.
(11) Zuleta, J. A.; Chesta, C. A.; Eisenberg, R. *J. Am. Chem. Soc.* **1989**, *111*, 8916.
(12) Zuleta, J. A.; Burberry, M. S.; Eisenberg, R. *Coord. Chem. Rev.* **1990**, *97*, 47.
(13) Zuleta, J. A.; Bevilacqua, J. M.; Eisenberg, R. *Coord. Chem. Rev.* **1991**, *111*, 237.
(14) Zuleta, J. A.; Bevilacqua, J. M.; Rehm, J. M.; Eisenberg, R. *Inorg. Chem.* **1992**, *31*, 1332.
(15) Bevilacqua, J. M; Zuleta, J. A.; Eisenberg, R. *Inorg. Chem.* **1994**, *33*, 258.
(16) Bevilacqua, J. M; Eisenberg, R. *Inorg. Chem.* **1994**, *33*, 1886.
(17) Zuleta, J. A.; Bevilacqua, J. M.; Proserpio, D. M.; Harvey, P. D.; Eisenberg, R. *Inorg. Chem.* **1992**, *31*, 2396.
(18) Bevilacqua, J. M; Eisenberg, R. *Inorg. Chem.* **1994**, *33*, 2913.
(19) (a) Cummings, S. D.; Eisenberg, R. *Inorg. Chem.* **1995**, *34*, 2007. (b) Cummings, S. D.; Eisenberg, R. *J. Am. Chem. Soc.* **1996**, *118*, 1949.
(20) Wootton, J. L.; Zink, J. I. *J. Phys. Chem.* **1995**, *99*, 7251.
(21) Vogler, A.; Kunkely, H. *J. Am. Chem. Soc.* **1981**, *103*, 1559.
(22) Puthraya, K. H.; Srivastava, T. S. *J. Ind. Chem. Soc.* **1985**, *62*, 843.
(23) Puthraya, K. H.; Srivastava, T. S. *Polyhedron* **1985**, *4*, 1579.
(24) Shukla, S.; Kamath, S. S.; Srivastava, T. S. *J. Photochem. Photobiol., A: Chem.* **1989**, *50*, 199.

S0020-1669(96)00685-4 CCC: $12.00

On the basis of this finding it was hypothesized that the photochemical reaction involved oxidation of the dithiolate ligand by $^1O_2{}^*$ in a manner consistent with the reactivity of organic thioethers.[22−24]

Recent elegant studies by M. Darensbourg and co-workers on the course of thermal and photochemical oxidation of Ni(II) and Pd(II) complexes featuring N_2S_2 coordination spheres provide considerable insight into possible pathways for the photoreactivity of $(NN)Pt^{II}(SS)$ complexes reported by Srivastava's group.[25−28] First, Darensbourg's group demonstrated that metal−sulfinate and −sulfenate complexes ($M[S(O)_2R]$ and M[SOR], respectively) derived from thermal oxidation and photooxidation of the corresponding thiolate complexes are stable and can be fully characterized (including X-ray structures in many cases). Furthermore, through a series of product and mechanistic studies they show that the reactivity of sulfur in the nickel(II) and palladium(II) dithiolates is remarkably similar to that of sulfur in thioethers.[29−31] Thus, reaction pathways to metal−sulfinate and −sulfenate complexes appear to be congruent with the pathways for photooxidation and thermal oxidation of organic thioethers to sulfonates and sulfoxides ($RS(O)_2R$ and RSOR, respectively).

Our group has been studying the photophysics of MLCT and LLCT excited states in transition metal complexes.[32−36] During the course of routine photophysical studies on $(tbubpy)Pt^{II}(dpdt)$ and $(tbubpy)Pt^{II}(edt)$ (**1** and **2**, respectively, where tbubpy = 4,4′-di-*tert*-butyl-2,2′-bipyridine, dpdt = *meso*-1,2-diphenyl-1,2-ethanedithiolate, and edt = 1,2-ethanedithiolate) we discovered that the two complexes were moderately photochemically reactive in air-saturated solution. Given the previous work in the area,[22−24] we were not surprised by the photosensitivity of **1** and **2** in the presence of dioxygen; however, we were intrigued by preliminary results which suggested that **1** and **2** react via different pathways. Thus, we embarked on a study of the photophysics and photoreactivity of the two complexes in an effort to ascertain the reaction products and the pathways by which they form. The mechanistic and product studies reported herein imply that the photoreactivity of both complexes arises from a primary step involving energy transfer from the charge transfer to diimine excited state Pt(II) complex to dioxygen to produce singlet oxygen ($^1O_2{}^*$) which then reacts with the dithiolate ligand in the ground state complex. The overall course of the reaction of edt complex **2** with $^1O_2{}^*$ is remarkably similar to that reported by Darensbourg and co-workers for Ni(II) and Pd(II) dithiolate complexes.[25−28] In contrast, the reactivity of dpdt complex **1** with $^1O_2{}^*$ is unique and apparently stems from a difference in the secondary reactions undergone by the primary adduct formed by initial attack of $^1O_2{}^*$ on the ground state complex.

Experimental Section

General Synthetic Data. Solvents and chemicals used for synthesis were of reagent grade and were not purified unless noted otherwise. NMR spectra were obtained on either GE QE-300 or Varian Gemini 300 MHz spectrophotometers. K_2PtCl_4 was obtained from Aldrich Chemical Company and used as received. 4,4′-Di-*tert*-butyl-2,2′-bipyridine was prepared by coupling 4-*tert*-butylpyridine over 10% Pd/C,[37] $(tbubpy)PtCl_2$ was prepared by reaction of K_2PtCl_4 with tbubpy,[38] and *fac*-$(tbubpy)Re^I(CO)_3Cl$ (**3**) was prepared from tbubpy and $Re(CO)_5Cl$.[36]

(4,4′-Di-*tert*-butyl-2,2′-bipyridine)(*meso*-1,2-diphenyl-1,2-ethanedithiolato)platinum(II) (1). Compound **1** was prepared by reaction of $(tbubpy)PtCl_2$ with *meso*-1,2-diphenyl-1,2-ethanedithiolate (dpdt) by analogy to literature methods.[19b] The dpdt ligand was prepared in three steps from *trans*-stilbene oxide according to the method of Overberger and Druker.[39] Under a nitrogen atmosphere, 30 mL of an ethanol solution containing 92 mg of dpdt (0.34 mmol) and 80 mg of NaOH (2 mmol) was mixed with 20 mL of an acetone solution containing 102 mg of $(tbubpy)PtCl_2$ (0.19 mmol). A red precipitate formed immediately upon mixing. The resulting suspension was stirred for 1 h, whereupon the volume of the solvent was reduced to 20 mL under reduced pressure. Then 40 mL of diethyl ether was added to the mixture, the red solid was collected by filtration on a medium porosity fritted funnel, and it was washed with excess ether. The product was obtained as a blood-red powdery solid, yield 107 mg (80%). ^1H NMR ($CDCl_3$): δ 1.43 (s, 18H), 4.45 (s, 2H, satellite peaks are observed for coupling to ^{195}Pt), 7.06 (m, 6H), 7.32 (m, 4H), 7.43 (dd, 2H), 7.94 (d, 2H), 9.22 (d, 2H, satellite peaks are observed for coupling to ^{195}Pt). ^1H NMR (CD_3CN): δ 1.43 (s, 18H), 4.34 (s, 2H, satellite peaks are observed for coupling to ^{195}Pt), 7.04 (m, 6H), 7.34 (m, 4H), 7.60 (dd, 2H, $J_1 = 2$ Hz, $J_2 = 6$ Hz), 8.29 (d, 2H, $J = 2$ Hz), 8.99 (d, 2H, $J = 6$ Hz, satellite peaks are observed for coupling to ^{195}Pt). HRMS (FAB, positive ion): calcd for $C_{32}H_{36}N_2S_2Pt$, 707.1968; obsd, 707.2016.

(4,4′-Di-*tert*-butyl-2,2′-bipyridine)(ethanedithiolato)platinum-(II) (2). This compound was prepared from $(tbubpy)PtCl_2$ and 1,2-ethanedithiol according to literature methods.[19] ^1H NMR ($CDCl_3$): δ 1.44 (s, 18H), 2.50 (s, 4H), 7.48 (d, 2H), 7.85 (d, 2H), 9.17 (dd, 2H). HRMS (FAB, positive ion): calcd for $C_{20}H_{28}N_2S_2Pt$, 555.1342; obsd, 555.1374.

Steady-State Photochemistry: Product Studies. Experiments aimed at determining the products of the photochemical processes were carried out using a 450-W medium-pressure Hanovia lamp that was contained within a water-cooled Pyrex immersion well. The 366 nm mercury emission from the arc lamp was isolated by placing Corning 7-54 and Schott LG 350 glass filters between the sample and the Hanovia lamp. Photolysis of **1** or **2** was carried out by dissolving approximately 3 mg of the complex in 10 mL of CH_3CN. The (air-saturated) solution was placed in a Pyrex test tube and placed approximately 6 in. from the filtered Hanovia lamp. The extent of reaction was followed by monitoring the UV−visible absorption spectrum. Irradiation was discontinued when UV−visible absorption showed that >90% of the starting material had disappeared (approximately 10 min of total photolysis time was usually required). The solvent was then removed under reduced pressure. The product from photolysis of **2** was not sufficiently soluble for NMR analysis. Solid samples of both photoproduct mixtures were submitted for mass spectral analysis.

Photoproduct from 1. ^1H NMR ($CDCl_3$): δ 1.24 (s, 9H), 7.08 (m, 10 H), 7.25 (d, 2H), 8.17 (s, broad, 2H), 8.49 (d, 2H). HRMS (FAB, nitrobenzyl alcohol matrix, positive ion): calcd for $C_{32}H_{34}PtN_2S_2$, 705.1812; obsd, 705.1811.

(25) Mills, D. K.; Reibenspies, J. H.; Darensbourg, M. Y. *Inorg. Chem.* **1990**, *29*, 4364.
(26) Tuntulani, T.; Musie, G.; Reibenspies, J. H.; Darensbourg, M. Y. *Inorg. Chem.* **1995**, *34*, 6279.
(27) Darensbourg, M. Y.; Tuntulani, T.; Reibenspies, J. H. *Inorg. Chem.* **1995**, *34*, 6287.
(28) Grapperhaus, C. A.; Darensbourg, M. Y.; Sumner, L. W.; Russell, D. H. *J. Am. Chem. Soc.* **1996**, *118*, 1791.
(29) Liang, J.-J.; Gu, G.-L.; Kacher, M. L.; Foote, C. S. *J. Am. Chem. Soc.* **1983**, *105*, 4717.
(30) Watanabe, Y.; Kuriki, N.; Ishiguro, K.; Sawaki, Y. *J. Am. Chem. Soc.* **1991**, *113*, 2677.
(31) Clennan, E. I.; Zhang, H. *J. Org. Chem.* **1994**, *59*, 7952.
(32) Wang, Y.; Hauser, B. T.; Rooney, M. M.; Burton, R. D.; Schanze, K. S. *J. Am. Chem. Soc.* **1993**, *115*, 5675.
(33) Wang, Y.; Lucia, L. A.; Schanze, K. S. *J. Phys. Chem.* **1994**, *99*, 1961.
(34) Lucia, L. A.; Wang, Y.; Nafisi, K.; Netzel, T. L.; Schanze, K. S. *J. Phys. Chem.* **1995**, *99*, 11801.
(35) Lucia, L. A.; Whitten, D. G.; Schanze, K. S. *J. Am. Chem. Soc.* **1996**, *118*, 3057.
(36) Wang, Y.; Schanze, K. S. *J. Phys. Chem.* **1996**, *100*, 5408.
(37) Cook, M. J.; Lewis, A. P.; McAuliffe, G. S. G.; Skarda, V.; Thomsen, A. J.; Glaspar, J. L.; Robbins, D. J. *J. Chem. Soc. Perkin Trans. 2* **1984**, 1293.
(38) Hodges, K. D.; Rund, J. V. *Inorg. Chem.* **1975**, *14*, 525.
(39) Overburger, C. G.; Drucker, A. *J. Org. Chem.* **1964**, *29*, 360.

Photoproducts from 2. HRMS (FAB, nitrobenzylalcohol matrix, positive ion): calcd for $C_{20}H_{28}PtN_2S_2O_2$, 587.1240; obsd, 587.1282; calcd for $C_{20}H_{28}PtN_2S_2O_3$, 603.1190; obsd, 603.1185; calcd for $C_{20}H_{28}PtN_2S_2O_4$, 619.1139; obsd, 619.1156. IR(KBr), ν(SO) (cm^{-1}): 901, 912, 1062, 1210.

Mechanistic Photochemical Studies. Quantum yield studies were carried out by using a 75-W high-pressure mercury short arc lamp housed in an elliptical reflector housing (Photon Technology International, Model ALH-1000). The output of the high-pressure arc lamp was passed through a grating monochromator and then focused into a small sample holder box. The sample was contained in a 1 × 1 cm cuvette and was stirred continuously during photolysis. The light intensity was calibrated at least one time each day by using the Aberchrome 540 actinometer (typical intensity was 1.0×10^{-8} einstein s^{-1}). Conversion efficiencies for complex **1** were determined by HPLC analysis on a system comprised of a two-pump gradient system controlled by a Macintosh SE computer (Rainin Instruments). Separations were performed on a C_{18} reversed phase column (Rainin Microsorb-MV) eluting with a 75% CH_3CN/H_2O mobile phase. Quantum yields for disappearance of **1** were determined by comparing the HPLC peak area for the complex with that of an internal standard (naphthalene). Conversion efficiencies for complex **2** were determined by UV−visible absorption spectroscopy, since the photochemical products were nonabsorbing.

Relative photochemical kinetics were carried out with the same arc lamp system used for the quantum yield studies. Aliquots (3.0 mL) of the solutions were placed in 1 × 1 cm quartz UV−visible absorption cells and exposed to 436 nm light from the high-pressure Hg arc lamp. Relative rates of conversion were determined by monitoring the UV−visible absorption of the solutions as a function of light exposure time.

Photophysical Experiments. Absorption spectra were obtained on a HP-8452A diode array spectrophotometer. Steady-state emission spectroscopy was carried out on a SPEX F-112 photon-counting spectrofluorimeter. Luminescence quantum yields are reported relative to $Ru(bpy)_3^{2+}$ in H_2O ($\Phi_{em} = 0.055$).[40] Low-temperature emission spectra were obtained on samples contained in a finger dewar that was filled with liquid N_2. Fluorescence lifetimes were obtained by time-correlated single photon counting (FLI, Photochemical Research Associates). Transient absorption spectroscopy was carried out on an instrument that has been fully described in the literature.[41a] Samples were excited by using the third harmonic output of a Q-switched Nd:YAG laser (10 ns fwhm, 10 mJ/pulse). For transient absorption studies sample solutions were contained in a recirculating cell (sample pathlength 1 cm) that held a 100 mL total volume in order to minimize the effects of photolysis during data acquisition. Degassing was effected by bubbling with argon. Multiwavelength transient absorption kinetics were analyzed by factor analysis methods using SPECFIT.[41b,c]

Results and Discussion

Absorption and Luminescence Spectroscopy. At the outset we note that the absorption and luminescence properties of edt complex **2** were previously studied by Eisenberg and co-workers and all of the data presented herein for this complex compare favorably with their report.[19b] The properties of **2** were examined in the present study in order to facilitate comparison with data obtained on **1**, which has not been previously studied.

Figure 1 illustrates the near-UV and visible absorption spectra of **1** and **2** in CH_3CN solution and Table 1 contains a listing of the absorption bands and extinction coefficients. For both complexes the low energy region of the spectrum is dominated by a moderately intense charge transfer absorption band. This transition has previously been assigned to arise from a charge transfer configuration in which the donor (HOMO) orbital is predominantly of $Pt(S)_2$ character and the acceptor (LUMO) orbital is dominated by π^* tbubpy (i.e., $Pt(S)_2 \rightarrow$ tbubpy CT).[17,20]

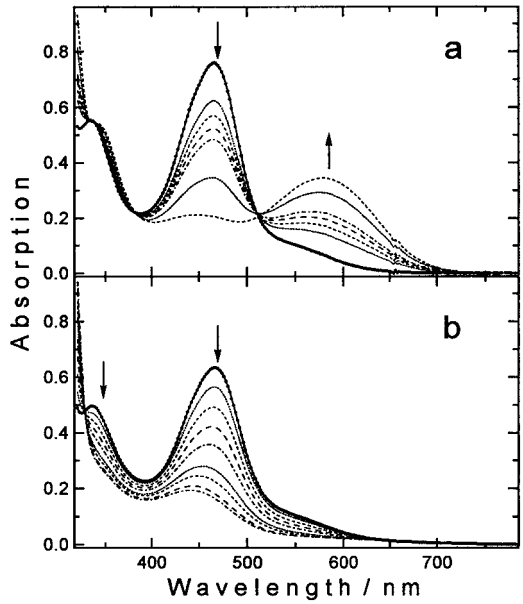

Figure 1. UV−visible absorption spectra as a function of irradiation time in air-saturated CH_3CN solution. Solid lines with point markers are spectra prior to irradiation. Arrows indicate direction of change of spectra with increasing light exposure. Key: (a) complex **1**; (b) complex **2**.

Table 1. UV−Visible Absorption Spectra and Assignments[a]

λ_{max}/nm (ϵ_{max}/M^{-1} cm^{-1})		
complex **1**	complex **2**	assignment
560 sh (740)	560 sh (790)	$Pt(S_2) \rightarrow$ tbubpy LLCT/MLCT
466 (6190)	466 (5420)	$Pt(S_2) \rightarrow$ tbubpy LLCT/MLCT
336 sh (4120)	336 sh (3800)	$Pt \rightarrow$ tbubpy MLCT
296 (17200)	296 (16000)	π,π^* tbubpy

[a] CH_3CN solution at 298 K. Estimated error in λ_{max} is ±2 nm and in ϵ_{max} is ±5%.

The absorption spectra of **1** and **2** are nearly indistinguishable, indicating that the 1,2-diphenyl substituents in the dpdt ligand have little effect upon the electronic structure of the charge transfer chromophore. This is not surprising, given that the phenyl groups in **1** are not conjugated with the thiolate donors.

An interesting feature is the shoulder appearing on the low-energy side of the $Pt(S)_2 \rightarrow$ tbubpy charge transfer transition. This shoulder clearly signals the existence of a low-energy transition having approximately $^1/_{10}$th the oscillator strength of the stronger (spin allowed) CT band which is at higher energy. The low energy transition is Stokes-shifted to a relatively small extent from the emission of **1** and **2** in a low-temperature glass (*vide infra*). Since the emission is clearly from a state having predominantly triplet spin character,[19b] it is likely that the low energy shoulder observed in the absorption spectra of **1** and **2** may be the corresponding singlet → triplet ($Pt(S)_2 \rightarrow$ tbubpy) (spin forbidden) charge transfer transition.

Steady-state and time-resolved luminescence studies were carried out on **1** and **2** to compare their luminescence properties (Table 2). Both complexes emit weakly at 298 K in CH_3CN solution, consistent with the reports of luminescence from structurally similar $(NN)Pt^{II}(SS)$ complexes by Eisenberg and co-workers.[19b] Emission from **1** is slightly more efficient than that of edt complex **2** as reflected by the slightly larger luminescence quantum efficiency (Φ_{em}) for the former. The emission of **2** at 298 K is also slightly red-shifted compared to that of **1**. Emission spectra were recorded for **1** and **2** in a 4:1 EtOH/MeOH glass at 77 K and λ_{max} values are reported in Table 2. The low temperature emission of the two complexes is virtually superimposable and is strongly blue-shifted compared

(40) Harriman, A. *J. Chem. Soc., Chem. Commun.* **1977**, 777.
(41) (a) Wang, Y.; Schanze, K. S. *Chem. Phys.* **1993**, *176*, 305. (b) SPECFIT, version 2.10. Spectrum Software Associates, Chapel Hill, NC, 1996. (c) Stultz, L. K.; Binstead, R. A.; Reynolds, R. A.; Meyer, T. J. *J. Am. Chem. Soc.* **1995**, *117*, 2520.

Table 2. Photophysical Properties of Platinum Complexes[a]

compound	λ_{max}/nm (77 K) [b]	Φ_{em}	τ_{em}/ns	τ_{em}^{air}/ns	η_q^{*Pt}	k_r/s^{-1}	k_{nr}/s^{-1}
1	770 (623)	0.0010	18.7	14.9	0.20	5.6×10^4	5.6×10^7
2	785 (623)	0.00036	7.0	6.2	0.11	4.6×10^4	1.3×10^8

[a] Data for CH_3CN solutions at 298 K unless otherwise indicated. [b] Value in parentheses is emission maximum at 77 K in 4:1 EtOH/MeOH.

to the emission at 298 K. This luminescence rigidochromism has been reported by Eisenberg for other (NN)Pt^{II}(SS) complexes[19] and is typical for charge transfer luminescence for metal−organic complexes.[2,42]

Emission lifetimes were determined for **1** and **2** in argon-degassed and air-saturated CH_3CN solutions (τ_{em} and τ_{em}^{air}, respectively, Table 2). The emission lifetimes are comparatively short for both complexes; however, τ_{em} for **1** is slightly longer than that for **2**. The emission lifetimes for **1** and **2** are shorter in air-saturated solutions, indicating that O_2 quenches the luminescent excited state. Assuming that the concentration of O_2 is 1.9 mM in air-saturated CH_3CN at 298 K,[43] the second order rate constant for oxygen quenching, $k_q^{O_2}$ is 7.2×10^9 M^{-1} s^{-1} and 9.7×10^9 M^{-1} s^{-1} for **1** and **2**, respectively. (The mechanism for the oxygen quenching is discussed below.) The emission lifetime data can also be used to estimate the fraction of the charge transfer to diimine excited state that is quenched by O_2 (η_q^{*Pt}), eq 1. Calculated values for η_q^{*Pt} are listed in Table 2.

$$\eta_q^{*Pt} = 1 - \frac{\tau_{em}^{air}}{\tau_{em}} \quad (1)$$

Assuming that the luminescent excited state is populated with unit efficiency following photoexcitation, it is possible to calculate the radiative and nonradiative decay rates (k_r and k_{nr}, respectively) from the emission data by eqs 2 and 3, where the

$$k_r = \frac{\Phi_{em}}{\tau_{em}} \quad (2)$$

$$k_{nr} = \left(\frac{1}{\tau_{em}}\right)[1 - \Phi_{em}] \approx \frac{1}{\tau_{em}} \quad (3)$$

approximation on the right hand side of eq 3 holds for **1** and **2** because $\Phi_{em} \ll 1$. The values of k_r and k_{nr} for **1** and **2** listed in Table 2 are in accord with those previously reported for (NN)-Pt^{II}(SS) complexes.[19b] In both cases $k_{nr} \gg k_r$, and therefore excited state decay is dominated by nonradiative pathways.

Photochemical Product Studies. Irradiation of deoxygenated CH_3CN solutions of complexes **1** or **2** at 436 nm for extended periods of time did not induce observable changes in their UV−visible absorption spectra or HPLC chromatograms. Thus, both complexes are photostable in the absence of oxygen. In contrast, irradiation of air-saturated solutions of both complexes at 436 nm led to relatively rapid changes in their UV−visible absorption spectra (Figure 1). First, for complex **1** in air-saturated CH_3CN, 436 nm photolysis leads to bleaching of the 466 nm charge transfer absorption band with concomitant development of a new absorption band with $\lambda_{max} \approx 582$ nm. Isosbestic points are maintained during the photolysis at 336, 382, and 512 nm. The spectral changes observed during photolysis of **1** are indicative of a clean photochemical reaction giving rise to a single visible region absorbing product. Irradiation of **2** in air-saturated CH_3CN at 436 nm gives rise to relatively uniform bleaching of the near-UV and visible absorption of the complex. No new absorption bands are observed in the near-UV and visible regions.

In order to provide further information concerning the products produced by irradiation of **1** and **2** in air-saturated solution, semipreparative photochemical studies were carried out. These experiments were rendered difficult due to poor solubility of **1** and **2** and the photoproduct mixtures. For both complexes, samples were photolyzed as dilute, air-saturated CH_3CN solutions with the 366 nm output of a medium-pressure Hg arc. After photolysis, the solvent was removed under reduced pressure. For complex **1** the photoproduct residue was sufficiently soluble in $CDCl_3$ to allow ^1H NMR analysis; however, the photoproduct from **2** was not sufficiently soluble in any common solvent to allow NMR analysis. Photoproducts from both samples were analyzed by high-resolution mass spectrometry (HRMS) using fast atom bombardment (FAB) as the ionization method.

The ^1H NMR spectrum of the photoreaction mixture from **1** reveals a single major photoproduct with aromatic region resonances for the tbubpy ligand at $\delta = 7.25$ (3,3′-tbubpy), 8.17 (5,5′-tbubpy), and 8.49 (6,6′-tbubpy) ppm. The corresponding protons in the starting material (**1**) exhibit resonances at $\delta =$ 7.43 (3,3′-tbubpy), 7.94 (5,5′-tbubpy), and 9.22 (6,6′-tbubpy) ppm. The interesting feature is that the resonances for the 3,3′ and 6,6′ protons are shifted upfield in the photoproduct compared to their shifts in **1**. Since these protons are located on the carbons with the largest coefficient for the π^* orbital of the tbubpy ligand,[17] they are the most sensitive to effects of π backbonding with Pt. Thus, the upfield shifts observed for the 3,3′ and 6,6′ protons in the photoproduct indicate stronger Pt → tbubpy π-back-bonding in the photoproduct or alternatively that the $Pt(S)_2$ unit is a stronger electron donor in the photoproduct. Note that this is consistent with the UV−visible absorption spectral changes, which indicate that the low energy charge transfer to diimine absorption band in the photoproduct is at longer wavelength than in **1**.

The most revealing information concerning the structure of the photoproduct obtained from **1** is the high resolution mass spectrum. The spectrum is dominated by a peak cluster centered at *m*/*e* 705.1812, which is in excellent agreement with the molecular formula $C_{32}H_{34}PtN_2S_2$. This formula corresponds to **1** minus two hydrogens.

Taken together, the spectroscopic information obtained on the photoproduct of **1** is consistent with the photochemical reaction in eq 4. The UV−visible absorption band ($\lambda_{max} \approx 582$ nm) and proton NMR chemical shifts for the tbubpy ligand in the photoproduct are consistent with the greater degree of delocalization and stronger electron donor properties of the Pt-$(S)_2$ unit in **4** compared to **1**. Indeed, λ_{max} for the visible absorption band for photoproduct **4** (582 nm) is relatively close

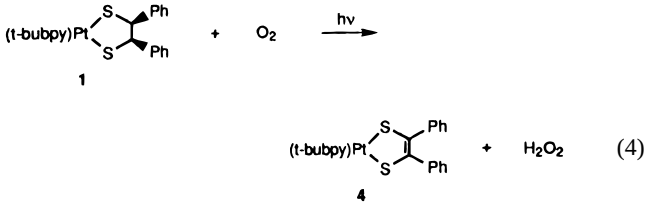

(4)

(42) (a) Lumpkin, R. S.; Meyer, T. J. *J. Phys. Chem.* **1986**, *90*, 5307. (b) Lees, A. J. *Chem. Rev.* **1987**, *87*, 711.
(43) Murov, S. L.; Carmichael, I.; Hug, G. L. *Handbook of Photochemistry*, 2nd ed.; Marcel Dekker: New York, 1993.

to the absorption maximum of the structurally similar complex (tbubpy)Pt(tdt) (tdt = 3,4-toluenedithiolate) which is λ_{max} = 567 nm in CH_2Cl_2.[19b]

Relatively less spectroscopic information is available concerning the photoproduct produced by irradiation of edt complex **2**. As noted above, photolysis of **2** is accompanied by relatively uniform bleaching of the visible charge transfer absorption bands typical of the $(NN)Pt^{II}(SS)$ chromophore. This observation strongly implies that a dehydrogenation reaction analogous to that observed for **1** does not occur. Unfortunately, the product mixture obtained from **2** was not sufficiently soluble to allow NMR analysis. However, the high resolution mass spectrum provides information that is strongly suggestive of the structure of the major photoproducts. The HRMS of the photoproduct is dominated by three peak clusters which appear at *higher m/e* compared to that of **2**. These peaks appear at m/e values of 587.1282, 603.1185 and 619.1156 and they correspond, respectively, to the molecular formulas $C_{20}H_{28}N_2S_2O_2Pt$, $C_{20}H_{28}N_2S_2O_3Pt$, and $C_{20}H_{28}N_2S_2O_4Pt$. In other words, the major photoproducts appear to result from addition of 1, 1.5, or 2 equiv of O_2 to starting complex **2**.

In view of the UV−visible absorption and HRMS data for photolysis of **2**, we suggest that the photoreaction involves oxygenation of the thiolate ligand as illustrated in eq 5; e.g.,

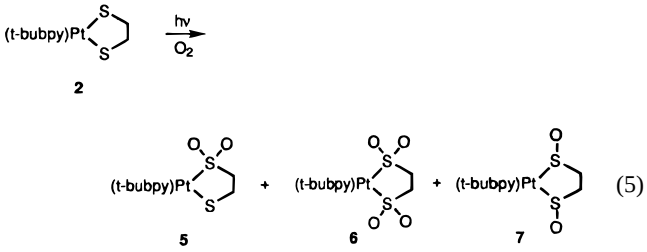

(5)

the product complexes contain sulfinate (SO_2R) or sulfenate (SOR) ligands. Several lines of evidence support this mode of reactivity. First, very similar reactivity has been reported by Darensbourg and co-workers for thermal and photochemical oxidation of Ni(II) and Pd(II) dithiolate complexes (*vide infra*).[25−28] Second, structures **5**−**7** are consistent with the UV−visible absorption data, since the sulfinate and sulfenate ligands are expected to be poorer electron donors compared to thiolate, thereby shifting the charge transfer to diimine absorption to higher energy. Finally, the presence of sulfinate and sulfenate functionality in the photoproducts is confirmed by IR spectroscopy of the reaction mixture which features moderately intense bands at 901, 912, 1062, and 1210 cm^{-1}. Assignment of the ν(SO) IR bands in the photoproduct mixture is based on previous work which reveals that nickel(II) and palladium(II) sulfinate complexes display bands for asymmetric and symmetric SO stretching at approximately 1050 and 1180 cm^{-1}, respectively. The corresponding palladium(II) bis(sulfenate) complexes (e.g., $Pd^{II}[(SOR)]_2$) display two closely spaced bands at 910 and 930 cm^{-1}. In view of this data, it appears as though the 1062 and 1210 cm^{-1} bands in the **1** photoproduct mixture correspond to sulfinate products (**5** and/or **6**) while the closely spaced "doublet" at 901 and 912 likely corresponds to the bis(sulfenate) complex **7**.

Mechanistic Photochemical Pathways. As noted in the Introduction, a recent series of reports describes the course of thermal and photochemical oxidation of Ni(II) and Pd(II) complexes featuring N_2S_2 coordination spheres.[25−28] This work provides considerable insight into possible mechanistic pathways for photooxidation of **1** and **2**. In general, the reactivity of sulfur in Ni(II) and Pd(II) dithiolates is similar to that of sulfur in thioethers.[29−31] Thus, reaction pathways to metal−sulfinate and −sulfenate complexes are believed to involve reactive intermediates **A** (a sulfoperoxide) and/or **B** (a thiadioxirane) which

Scheme 1

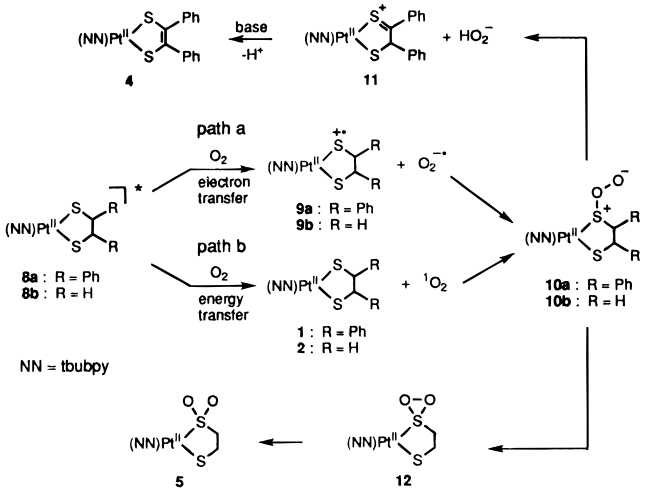

M = metal

are formed by reaction of the dithiolate complexes with ground state (triplet) or excited state (singlet) dioxygen ($^3O_2$ and $^1O_2$, respectively) or oxygen transfer agents such as H_2O_2.[26,27,44] Of most significance to the present study is the recent report that UV photolysis of $(NN)Pd^{II}(SS)$ (in this case NN = diamino) complexes in the presence of O_2 leads to product mixtures containing sulfinato, bis(sulfinato), and mixed sufinato and sulfenato ligands in the coordination sphere.[26] It has been suggested that the photoinduced reactions involve $^1O_2$ as the oxidant, although this point has not been examined in detail.[26]

Scheme 1 contains several mechanistic pathways that are consistent with the products observed in the photoreactions of **1** and **2** and are formulated based on the earlier studies of (photo)oxidation of metal dithiolates.[26,27] First, it is clear that the products arise from a primary photochemical step involving the interaction of the $Pt(S)_2 \rightarrow$ tbubpy CT excited state (**8**) with O_2. This interaction may result either in (a) electron transfer to form radical cation complex **9** and superoxide ($O_2^{-\bullet}$) or (b) energy transfer to form the ground state complex (**1** or **2**) and excited state (singlet) oxygen, $^1O_2$. Either pathway (electron transfer or energy transfer) likely leads to formation of the sulfoperoxide complex **10**, which we believe is the key reactive

(44) A mechanism for formation of bis(sulfenate) complex **7** from **2** that must be considered involves addition of dioxygen across the cis-sulfurs to produce intermediate **C**

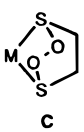

C

which may collapse directly to **7**. Evidence for such intermediates in the reaction between $^1O_2$ and nickel(II) thiolates has been presented.[28] At present we have not carried out a detailed study of the product distributions, rates of formation, etc, for oxygenation of **2** to delineate the pathways for formation of all of the possible products. Such studies are currently underway.

intermediate in the photoreaction.[44] Sulfoperoxide complex **10a**, which is formed from **1**, could decompose to **11** by loss of HO_2^- via intramolecular proton abstraction from the α-carbon by the oxyanion moiety. Cationic complex **11** then could lose a proton to a suitable base (i.e., HO_2^-) to form the observed dehydrogenation product **4**. In sulfoperoxide complex **10b**, deprotonation is slower (see below) and hence the complex collapses to sulfinate **5**, likely via thiadioxirane **12**. Although not explicitly shown in Scheme 1, it is likely that disulfinate complex **6** (eq 5) is formed by addition of a second equivalent of O_2 to **5**. Finally, although the mass spectrum of the photoproduct mixture from **2** reveals a peak cluster due to addition of three oxygens to the starting complex, it is not possible to rule out that this is a daughter ion formed by loss of O from disulfinate complex **6** in the gas phase. Previous mass spectroscopic studies (FAB ionization, NBA matrix) reveal that loss of one or more O atoms is a common mode of fragmentation in Ni(II) and Pd(II) sulfinate complexes.[27]

An interesting feature is the difference in the overall course of reaction for **1** and **2**. It is possible that this difference arises because of a difference in the reactivity of sulfoperoxide complexes **10a** and **10b**. The key step leading to dehydrogenation of **1** is likely decomposition of **10a** to **11** via loss of HO_2^-. This reaction probably involves intramolecular proton transfer as shown in eq 6. The fact that **10a** undergoes proton

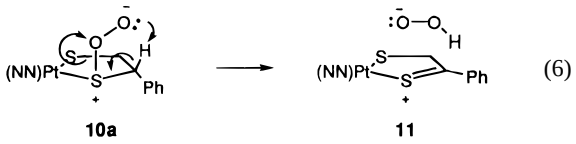

(6)

transfer and decomposition while **10b** simply collapses to thiadioxirane **12** is likely due to the fact that the phenyl substituent accelerates the rate of the intramolecular deprotonation step. This rate acceleration may result from a conformational effect of the phenyl group on the transition state for the deprotonation; the phenyl may force the metallacycle into a conformation where deprotonation is more facile. Alternatively, rate acceleration could simply arise because the phenyl substituent stabilizes the product of the decomposition (**11**).

A key question in the current study is whether the primary photochemical step involves electron transfer and superoxide ion (path a) or energy transfer and singlet oxygen (path b). The luminescence studies of **1** and **2** indicate that O_2 quenches the charge transfer to diimine excited state of both complexes at near the diffusion controlled rate. This rate of quenching is compatible with energy transfer (path b), since the charge transfer to diimine excited state of **1** and **2** lies some 0.6 eV above the energy of $^1O_2$ (i.e., energy transfer is exothermic by 0.6 eV). However, based on the estimated free energy change for electron transfer from the charge transfer to diimine excited state of **1** or **2** to O_2 ($\Delta G \approx -0.2$ eV),[45] we cannot rule out that quenching occurs by electron transfer (path a). Therefore, in an attempt to elucidate which pathway predominates, a series of mechanistic photochemical studies was performed.

Mechanistic Photochemical Studies. Quantum yields for disappearance (Φ_-) were determined for **1** and **2** in air-saturated CH_3CN solution for irradiation at 436 nm. For complex **1**, $\Phi_- = 0.13 \pm 0.04$ and is invariant within experimental error for concentrations ranging from 5×10^{-5} to 2×10^{-4} M. For complex **2** ($c = 1 \times 10^{-4}$ M) $\Phi_- = 0.05 \pm 0.01$. In both cases, the observed disappearance quantum yields are lower than the fraction by which O_2 quenches the charge transfer to the diimine excited state (η_q^{*Pt}, Table 2), indicating that irreversible photochemistry does not occur for each quenching encounter. However, nonproductive quenching could arise from either energy transfer or electron transfer pathways, and therefore, the quantum yield data alone does not distinguish either reaction pathway.

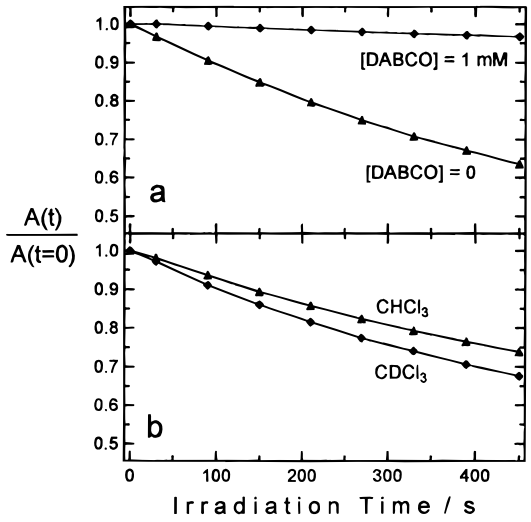

Figure 2. (a) Plot of $A(t)/A(t = 0)$ vs exposure time for solution of **1** in CH_3CN, where A = absorption at 463 nm. Plot marked with polygons: [**1**] = 0.2 mM and [DABCO] = 1.0 mM. Plot marked with triangles: [**1**] = 0.2 mM and [DABCO] = 0. (b) Plot of $A(t)/A(t = 0)$ vs exposure time for solution of **1**. Plot marked with triangles: $CHCl_3$ solvent. Plot marked with polygons: $CDCl_3$ solvent.

Next, a study of the effect of 1,4-diazabicyclo[2.2.2]octane (DABCO) on photooxidation of **1** in CH_3CN was carried out. DABCO was selected because it is an excellent quencher of $^1O_2$, but it does not interact with superoxide.[46,47] Prior to examining the effect of DABCO on the photoreaction, a Stern−Volmer luminescence lifetime quenching study was carried out to determine whether DABCO quenches the charge transfer to diimine excited state of **1**. This study revealed that, for [DABCO] ≤ 5 mM, lifetime quenching was not observed, placing an upper limit on the quenching rate constant of $k_q \leq 10^8\ M^{-1}\ s^{-1}$. The rate of photoinduced ($\lambda = 436$ nm) bleaching of the visible absorption band was determined for two air-saturated CH_3CN solutions of **1** ($c = 2 \times 10^{-4}$ M), one containing DABCO ($c = 1$ mM) and the other with no added DABCO. The results of this experiment are presented in Figure 2a as a plot of $A(t)/A(t = 0)$ vs exposure time, where A is the absorption at the charge transfer to diimine band maximum. It is quite clear from this figure that DABCO dramatically quenches the photoreaction: the initial slope of the plot with added DABCO is approximately a factor of 10 lower compared to that in the absence of DABCO. Since DABCO does not quench the charge transfer excited state of **1**, this experiment provides strong evidence that $^1O_2$ is involved in the photooxidation of **1**.

(45) On basis of the potential for the $O_2 + e^- \rightarrow O_2^{-\bullet}$ couple ($E° \approx -0.82$ eV vs SCE) and the excited state oxidation potential of **1** and **2** (i.e., $Pt^{*/+}$, $E° \approx -1.0$ V vs SCE), we estimate that electron transfer (path a) is exothermic by ca. 0.2 eV. The excited state potential of **1** is estimated from the excited state energy (1.6 eV) and the peak potential for the irreversible anodic oxidation (+0.6 V).

(46) (a) Bellus, D. in *Singlet Oxygen. Reactions With Organic Compounds and Polymers*; Ranby, B., Rabek, J. F., eds.; Wiley and Sons: New York, 1978; p 61. (b) Fee, J. A.; Valentine, J. S. In *Superoxide and Superoxide Dismutase*; Michelson, A. M., McCord, J. M., Fridovich, I., Eds.; Academic Press: New York, 1977; p 19.

(47) Kearns, D. R.; Merkel, P. B.; Nilsson, R. *J. Am. Chem. Soc.* **1972**, *94*, 7244.

A second experiment to test for the involvement of $^1O_2$ in the photooxidation reaction compared the relative photoreaction rate of **1** in air-saturated $CHCl_3$ and $CDCl_3$ solutions. Since the lifetime of $^1O_2$ is significantly longer in the deuterated solvent (300 μs in $CDCl_3$ vs 30 μs in $CHCl_3$),[47] it seemed likely that if $^1O_2$ is involved, the photoreaction will be more efficient in the deuterated solvent. Figure 2b illustrates the results of this experiment as a plot of $A(t)/A(t = 0)$ for bleaching of the charge transfer absorption band of **1** as a function of exposure time. As can be seen, this experiment indicates a slight, but reproducibly larger bleaching rate in the deuterated solvent, again consistent with the involvement of $^1O_2$.

Finally, since both kinetic studies pointed to the involvement of $^1O_2$ in the photoreaction of **1**, we rationalized that it should be possible to effect reaction by using methylene blue to sensitize the formation of $^1O_2$.[48] Thus, an air-saturated solution containing **1** ($c = 4 \times 10^{-4}$ M) and methylene blue ($c = 3.0 \times 10^{-4}$ M) was photolyzed with $\lambda > 600$ nm light from a medium-pressure mercury lamp. The long wavelength excitation insured that light was absorbed only by methylene blue. UV−visible absorption analysis of the solution during the course of the photolysis revealed uniform bleaching of the visible charge transfer absorption band of **1**, but without concomitant development of the long wavelength absorption band characteristic of the photooxidation product **4**.

Taken together, the mechanistic photochemical studies point to involvement of $^1O_2$ in the photooxidation of **1** (path B, Scheme 1). The result of the DABCO experiment is clear in that the reaction is suppressed almost entirely even at 1 mM concentration of the quencher. There is also a noticeable increase in reaction efficiency in $CDCl_3$, a result which is incompatible with the superoxide pathway.

Although the methylene blue experiment does not provide evidence for involvement of $^1O_2$ in the reaction of **1**, the fact that the dye does not act as a sensitizer does not preclude the involvement of $^1O_2$ in the self-sensitized reaction. This is because the visible absorption of **1** is uniformly bleached when the complex is photolyzed in the presence of the dye, which suggests that **1** may react directly with the triplet excited state of methylene blue ($^3MB^{+*}$). A distinct possibility is that **1** is oxidized by the triplet state of $^3MB^*$, e.g., $^3MB^{+*} + \mathbf{1} \rightarrow MB^{\bullet} + \mathbf{1}^{+\bullet}$; indeed, this electron transfer reaction is strongly exothermic ($\Delta G \approx -0.75$ eV).[49] An interesting point in this regard is that spectroelectrochemical studies demonstrate that anodic oxidation of **1** in CH_3CN solution (tetrabutylammonium perchlorate electrolyte) leads to uniform bleaching of the visible absorption of the complex, in a manner similar to that observed in the methylene blue sensitization reaction.

Transient Absorption Spectroscopy. Transient absorption spectroscopy was carried out on **1** and **2** in order to characterize the charge transfer excited state and to attempt to observe intermediates involved in the photooxidation reaction. All transient absorption studies were carried out with dilute solutions of the complexes ($c \approx 2 \times 10^{-4}$ M) in CH_3CN solvent with excitation at 355 nm.

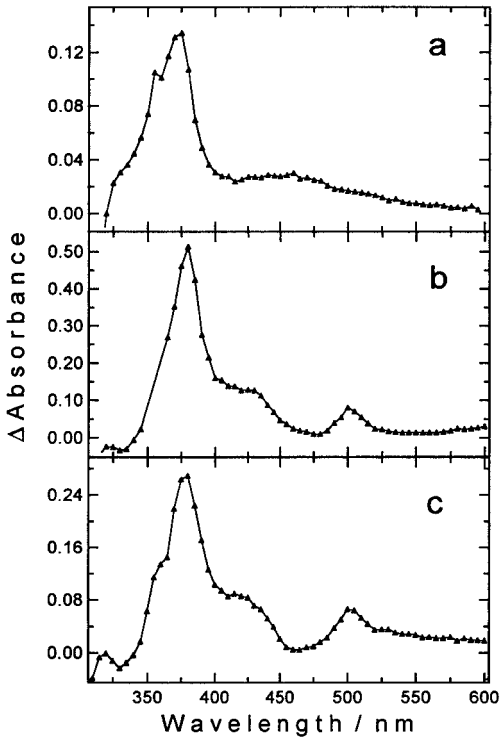

Figure 3. Transient absorption difference spectra following 355 nm pulsed laser excitation (10 mJ dose, 6 ns fwhm): (a) **3** in degassed CH_3CN, 10 ns delay after leading edge of laser pulse; (b) **1** in degassed CH_3CN, 5 ns delay after leading edge of laser pulse; (c) **2** in degassed CH_3CN, 5 ns delay after leading edge of laser pulse.

The first series of experiments was carried out to characterize the charge transfer to diimine excited states of **1** and **2**. Thus, the optical transients observed on the 0−500 ns time scale following laser excitation were closely examined. A parallel study was carried out on *fac*-(tbubpy)$Re^{I}(CO)_3Cl$ (**3**), which has a long-lived dπ (Re) → π^* (tbubpy) MLCT excited state.[50,51] Figure 3a illustrates the transient absorption spectrum of Re(I) complex **3** in degassed CH_3CN at 10 ns delay following laser excitation. This spectrum is dominated by a moderately intense absorption band in the near-UV region with $\lambda_{max} \approx 370$ nm, while broad, weak absorption extends throughout the visible region. The absorbing transient decays with a lifetime of 45 ns, in good agreement with the luminescence lifetime of the complex.[50] This correspondence indicates that the transient observed by laser flash photolysis is the luminescent excited state of **3**. The photophysics of luminescent complexes of the type (diimine)$Re^{I}(CO)_3Cl$ have been studied in great detail and the emissive state has been assigned as arising from a Re → diimine MLCT transition.[2,50,51] Thus, in a one-electron approximation, the excited state can be written as (tbubpy$^{-\bullet}$)$Re^{II}(CO)_3Cl$. The strong near-UV absorption feature observed in the transient absorption spectrum of **3** is likely due to a π,π^* or π^*,π^* transition of the tbubpy anion radical, (i.e., tbubpy$^{-\bullet}$), that is present in the MLCT state.[50−52]

Parts b and c of Figure 3 illustrate the transient absorption spectra of **1** and **2**, respectively, in degassed CH_3CN solution taken at a 5 ns delay relative to the leading edge of the laser excitation pulse. Within experimental error the spectra of the two complexes are the same, with the exception that the lifetimes of the transients observed for **1** and **2** are 27 and 10 ns,

(48) Turro, N. J. *Modern Molecular Photochemistry*; Benjamin/Cummings: Menlo Park, 1979.

(49) The free energy change for photoinduced electron transfer from **1** to triplet methylene blue, e.g., $^3MB^{+*} + \mathbf{1} \rightarrow MB^{\bullet} + \mathbf{1}^{+\bullet}$ is estimated by the equation $\Delta G = E_p(\mathbf{1}/\mathbf{1}^{+\bullet}) - E_{1/2}(MB^+/MB^{\bullet}) - E_{00}(^3MB^{+*})$, where $E_p(\mathbf{1}/\mathbf{1}^{+\bullet})$ is the peak potential for irreversible oxidation of **1** (+0.6 V), $E_{1/2}(MB^+/MB^{\bullet})$ is the half-wave reduction potential of methylene blue (0 V), and $E_{00}(^3MB^{+*})$ is the triplet energy of methylene blue (1.4 eV).

(50) Worl, L. A.; Duesing, R.; Chen, P.; Della Ciana, L.; Meyer, T. J. *J. Chem. Soc., Dalton Trans.* **1991**, 849.

(51) Lucia, L. A.; Burton, R. D.; Schanze, K. S. *Inorg. Chim. Acta* **1993**, *208*, 103.

(52) Watts, R. J. *J. Chem. Educ.* **1983**, *60*, 834.

respectively. The reasonably good correspondence between the emission and transient absorption lifetimes suggests that for both complexes the transient observed by flash photolysis is the emissive $Pt(S)_2 \rightarrow$ tbubpy charge transfer state. The transient absorption spectra of **1** and **2** are characterized by a strong near-UV band with $\lambda_{max} \approx 370$ nm and with weak absorption throughout the visible region. The band which appears at 500 nm may be an artifact resulting from the ground state bleaching which is clearly apparent in the spectra from 425 to 480 nm.

The interesting feature in Figure 3 is the close similarity between the transient absorption spectra of **1**, **2**, and **3**. Thus, the dominating feature in all three spectra is clearly due to the anion radical chromophore, tbubpy$^{\bullet -}$. The observation of this band in the excited state absorption spectra of **1** and **2** clearly supports the charge transfer to diimine assignment that has been previously made on the basis of solvatochromic effects, thermodynamic correlations and resonance Raman spectroscopy.[19−21] Unfortunately, absorption bands are not observed for the "radical cation" chromophore counterpart to tbubpy$^{-\bullet}$ (i.e., $Pt(S)_2^{+\bullet}$). However, given that the dithiolate ligands are saturated, strong absorption in the visible region is not anticipated for the $Pt(S)_2^{+\bullet}$ chromophore.

Next, a series of transient absorption studies were carried out on **1** and **2** in CH_3CN solution that was saturated with O_2 by purging with oxygen for 30 min. These experiments were carried out in an attempt to identify transients involved in the photooxidation process. First, transient absorption spectra of both complexes were obtained under conditions similar to those used to obtain the spectra shown in Figure 3 (i.e., delay times ranging from 0 to 500 ns following the laser excitation). For **1** and **2** the transient absorption spectra observed in O_2 saturated solution are *identical* to those in degassed solution, with the exception that the excited state decays more rapidly in the presence of O_2. Importantly, the transient absorption attributed to the charge transfer to diimine excited state decays to the baseline; that is, no long-lived bleaching or new transient absorption bands are observed on the 0−500 ns time scale after the charge transfer excited state decays. This observation clearly indicates that in the presence of O_2 the charge transfer excited state decays back to the ground state cleanly. If this were not the case, at the very least, long-lived bleaching would be observed in the region where the ground state absorbs. On the basis of this result, involvement of electron transfer and superoxide (path a) in the mechanism of the photooxidation reaction can be completely ruled out.

A final transient absorption experiment was carried out which provides definitive evidence that $^1O_2$ is responsible for the photooxidation reactions. In this experiment, a solution of **1** ($c = 2 \times 10^{-4}$ M) in O_2-saturated CH_3CN was subjected to laser flash photolysis and the transient absorption spectral changes were monitored on a time scale that ranged up to 50 μs after excitation. The results of this experiment are illustrated in Figure 4. Consistent with the studies carried out on the faster time scale, this experiment shows that at 800 ns delay following the laser pulse little or no transient absorption or ground state bleaching is apparent. However, over the 1−50 μs time scale, bleaching of the ground state absorption at $\lambda_{max} \approx 470$ nm occurs with concomitant development of a new absorption band with $\lambda_{max} \approx 570$ nm. Note that these spectroscopic changes are consistent with those observed in the absorption spectrum of **1** under steady state photolysis (Figure 1a). Therefore, this transient absorption data reveals that the reaction of **1** $\rightarrow$ **4** occurs on the 50 μs time scale following excitation. Furthermore, it implies that the reaction involves a nonabsorbing reactive intermediate which is produced as a result of the initial

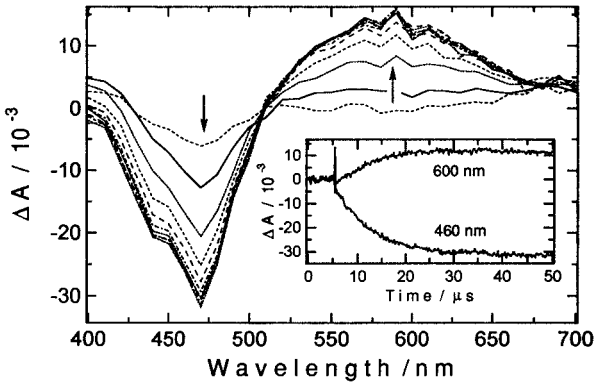

Figure 4. Transient absorption difference spectra following 355 nm pulsed laser excitation (20 mJ dose, 6 ns fwhm) of **1** in oxygen-saturated CH_3CN solution. Delay times range from 0.8 to 50 μs and arrows indicate direction of change with increasing delay. Inset: Transient absorption kinetics at 460 and 600 nm. Spike apparent at early time in the kinetic traces is due to the absorption of the short-lived charge transfer to diimine excited state.

laser excitation. This reactive intermediate must be $^1O_2$, which is reported to have a lifetime of 30 μs in CH_3CN.[47]

Figure 4 (inset) shows the kinetic traces for transient absorption data at 460 nm (bleaching of **1**) and 600 nm (absorption grow-in due to **4**). Inspection of this data reveals qualitatively that the kinetics of the bleaching and absorption increase are the same. Quantitative analysis of the transient absorption data using factor analysis[41b,c] shows that the bleach and absorption increase can be fitted with excellent statistics to a single (pseudo) first-order rate process with $k_{obs} = 9.3 \times 10^4$ s^{-1}. The fact that the rate of bleaching of the absorption of **1** and the grow-in of the absorption of **4** is the same indicates that the rate-determining step for the photooxidation reaction is the initial attack of $^1O_2$ on **1** to form sulfoperoxide **10a**. Apparently the subsequent reactions of **10a** $\rightarrow \rightarrow$ **4** are more rapid than formation of the sulfoperoxide. Assuming that the lifetime of $^1O_2$ is 30 μs,[47] it is possible to determine that the second-order rate constant for reaction between $^1O_2$ and **1** is $k_q^{^1O_2} = 3.0 \times 10^8$ M^{-1} s^{-1} and that at [**1**] = 0.2 mM the Pt complex quenches $^1O_2$ with an efficiency of $\eta_q^{^1O_2} = 0.65$.[53] Interestingly, the rate constant by which **1** and organic thioethers quench $^1O_2$ is very similar.[54] This is in keeping with the previously noted observation that the reactivity of metal dithiolate complexes and thioethers with oxygen transfer agents is similar.

Summary and Conclusions

Photolysis of (NN)Pt^{II}(SS) complexes **1** and **2** in air-saturated solution leads to a novel photooxidation reaction. Product and mechanistic studies indicate that this reaction involves $^1O_2$ as the active oxidizing agent. $^1O_2$ is produced by energy transfer from the luminescent charge transfer to diimine excited state

(53) The efficiency by which **1** quenches $^1O_2$ ($\eta_q^{^1O_2}$) is determined as follows. The observed rate for reaction of **1** (k_{obs}) in the laser flash photolysis is given by $k_{obs} = k_q^{^1O_2}$ [**1**] + $k_d^{^1O_2}$, where $k_q^{^1O_2}$ [**1**] is the pseudo-first-order rate constant for the quenching process and $k_d^{^1O_2}$ is the decay rate of $^1O_2$ in the absence of quencher. Now the quenching efficiency is given by $\eta_q^{^1O_2} = k_q^{^1O_2}$ [**1**]/($k_q^{^1O_2}$ [**1**] + $k_d^{^1O_2}$), which rearranges to $\eta_q^{^1O_2} = [1 - (k_d^{^1O_2}/k_{obs})]$. Substitution of $k_d^{^1O_2} = 3.3 \times 10^4$ s^{-1} and $k_{obs} = 9.3 \times 10^4$ s^{-1} into the latter equation yields $\eta_q^{^1O_2} = 0.65$.

(54) Foote, C. S. in *Singlet Oxygen*; Wasserman, H. H., Murray, R. W., eds.; Academic Press: New York, 1979; p 139.

of the $(NN)Pt^{II}(SS)$ complexes. While the overall course of the photooxidation reaction differs for **1** and **2**, the reaction is believed to involve a common sulfoperoxide intermediate that forms by attack of $^1O_2$ on the ground state dithiolate complex. Photooxidation of **1** and **2** is moderately efficient and appears to be general for $(NN)Pt^{II}(SS)$ complexes in air-saturated solution. The available kinetic data suggests that $^1O_2$ is produced with nearly unit efficiency by energy transfer from the charge transfer to diimine excited state; therefore the quantum efficiency for photooxidation is limited only by the efficiency of reaction between $^1O_2$ and the ground state $(NN)Pt^{II}(SS)$ complex.[55]

While the $(NN)Pt^{II}(SS)$ complexes exhibit properties that could be useful for application in solar energy conversion systems,[11−19] this study clearly demonstrates that use of these complexes in energy conversion would be limited to systems that operate anaerobically.

Acknowledgment. We gratefully acknowledge support for this project from the National Science Foundation (Grant No. CHE-9401620).

IC960685X

(55) As indicated in ref 53, at [**1**] = 0.2 mM, $\eta_q^{^1O_2} = 0.65$. Interestingly, $\eta_q^{^1O_2}$ is equivalent to the ratio of the quantum efficiency for disappearance of **1** to the efficiency for quenching of the charge transfer to diimine excited state by $^3O_2$ in air-saturated solution: $(\Phi_- / \eta_q^{*Pt}) = 0.64$. This correspondence implies that (a) $^1O_2$ is produced with unit efficiency when $^3O_2$ quenches the charge transfer to diimine state of **1** and (b) irreversible product formation (i.e., **1** → **4**) occurs with unit efficiency when **1** quenches $^1O_2$.